

Global and local synchrony of coupled neurons in small-world networks

Naoki Masuda¹ and Kazuyuki Aihara^{2,3}

¹ Faculty of Engineering, Yokohama National University, Yokohama, Japan

² Graduate School of Frontier Sciences, The University of Tokyo, Tokyo, Japan

³ ERATO, Japan Science and Technology Agency, Kawaguchi, Japan

Abstract

Synchronous firing of neurons is thought to play important functional roles such as feature binding and switching of cognitive states. Although synchronization has mainly been investigated using model neurons with simple connection topology so far, real neural networks have more complex structures. Here we examine behavior of pulse-coupled leaky integrate-and-fire neurons with various network structures. We first show that the dispersion of the number of connections for neurons influences dynamical behavior even if other major topological statistics are kept fixed. The rewiring probability parameter representing the randomness of networks bridges two spatially opposite frameworks: precise local synchrony and rough global synchrony. Finally, cooperation of the global connections and the local clustering property, which is prominent in small-world networks, reinforces synchrony of distant neuronal groups receiving coherent inputs.

1 Introduction

Synchronization of neurons is thought to play crucial roles in information processing in the brain. For example, the neurons sharing a common preferred stimulus fire synchronously when stimulated [9]. Switching between synchrony and asynchrony also occurs in response to modality changes during tasks [22]. Synchronously firing neurons may form a dynamical cell assembly to bind features such as visual objects [5, p. 145, 150], [7, 12, 29, 30]. Synchronous cell assemblies are robust against noise and can provide, by using the temporal dimension, a solution to the feature binding problem that involves combinatorial explosion [5, p. 142, 145]. In accordance, the mechanisms of synchronization and also those of desynchronization and clustered states have been explored using model neural networks with the complete couplings [26], random sparse couplings [8, 31], and local couplings [12, 24, 30].

However, the network topology considered in these works is too simple to give satisfactory answers to many basic questions. For example, all-to-all and random networks blur the information stored in local modules or individual neurons [24]. These architectures cannot explain the emergence of local clusters owing to relatively dense local couplings [20] while dynamic clusters formed by stimulus application or by internal dynamics may be essential elements in information processing [3]. Another deficiency of all-to-all couplings is that real neurons are usually more sparsely connected. On the other hand, locally connected networks are free from these shortcomings and can reproduce synchronization of different neural assemblies sharing a preferred stimulus as far as the assemblies are spatially close [12, 30]. However, slow information transmission via local connections can be an obstacle to binding remote objects, and real networks are likely to have much shorter pairwise distances than locally connected networks do.

Small-world networks [4, 32, 33] simultaneously realize dense local connections and short pairwise distances. These small-world properties are also found in biological neural networks [21, 23, 33]. In this paper we examine cooperative effects of local coupling, global coupling, and coherent inputs on synchronization.

The ordinary small-world networks and the methodologies in this study are explained in Sects. 2 and 3, respectively. Then we point out in Sect. 4 that the ordinary small-world networks are not appropriate for studying topological effects on dynamics of neural networks and introduce modified small-world networks. We next show in Sects. 5 and 6 that small-world networks enable two remote groups of neurons to synchronize when they receive coherent inputs. It is discussed in Sect. 7 that precise local synchrony and rough global synchrony are bridged by the rewiring probability specifying the randomness of networks.

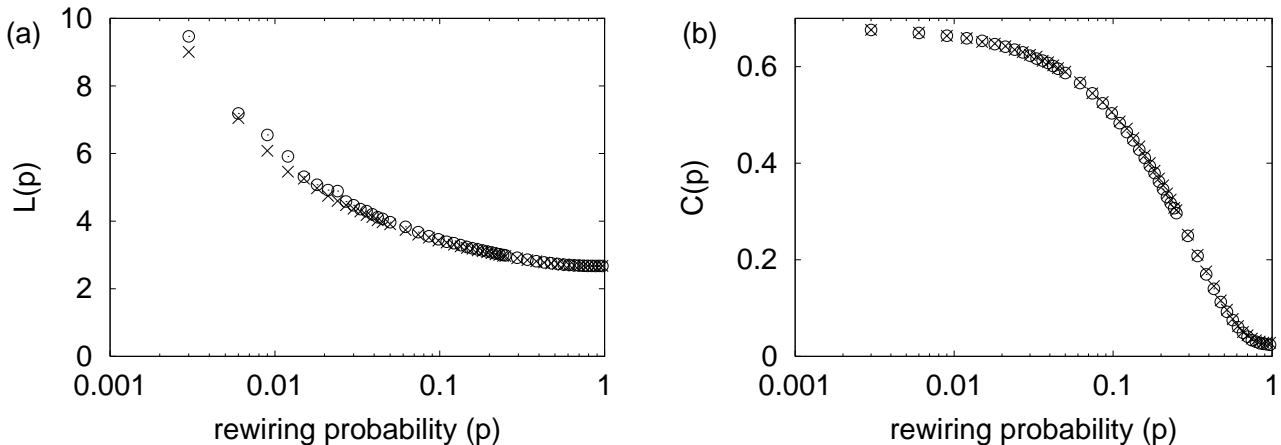


Figure 1: (a) $L(p)$ and (b) $C(p)$ for $n = 400$ and $k = 6$. The graphs are generated by the unbalanced random rewiring (crosses) and by the balanced random rewiring (circles).

2 Small-world Networks

The characteristic path length L and the clustering coefficient C are commonly used to quantify the distances between vertices and the clustering property, respectively [32, 33]. With a graph composed of n vertices, L is defined to be the shortest path length between two points averaged over all possible $n(n-1)/2$ pairs. On the other hand, a vertex with k_v neighbors could have at most $k_v(k_v-1)/2$ edges between pairs of the neighbors. The number of actual edges normalized by $k_v(k_v-1)/2$ and averaged over all the vertices gives C . Many real networks including social, ecological, and neural networks have small L and large C , whereas regular lattices have large L and large C and random sparse networks have small L and small C . Although all-to-all networks have small L and large C , they have unrealistically many edges.

To generate small-world networks with small L and large C , we prepare a ring of n vertices in which each vertex has $k/2$ nearest neighbors on each side [32, 33]. Then we rewire a fraction p of edges randomly by removing $pkn/2$ edges and creating $pkn/2$ new edges each of which leaves from the start point of a removed edge and ends at a randomly chosen vertex, avoiding multiple edges or recreation of the removed edges. As is shown in Fig. 1 for $n = 400$ (crosses), rewired graphs with $p \in [0.01, 0.1]$ have the small-world properties with small $L(p)$ and large $C(p)$. The regular lattice ($p = 0$) and the random graph ($p = 1$) are generated by this procedure as two extremes [32, 33]. Regarding neurobiology, the neural networks of *C. elegans* [33] and the connections between the cortex areas of macaque [21, 23] and cat [21] are reported to be in the small-world regime. Small-world networks may serve to reduce wiring costs compared with the all-to-all networks, to speed up information transmission compared with locally connected networks, and to preserve spatial information on signals in local assemblies in contrast to random networks. Small-world effects on synchronization have been explored with pulse-coupled integrators [10], Hodgkin-Huxley neurons [13, 14], and FitzHugh-Nagumo neurons [14]. However, the effect of heterogeneous k_v for nonzero p and that of the connection structures have not been distinguished. Furthermore, the relation between network topology and information processing with spatially heterogeneous inputs has not been discussed except in [14] that deals with localized inputs to trigger global synchrony and traveling waves. Therefore, using modified small-world networks introduced in Sect. 4, we focus on effects of coupling structure on the dynamics with spatially structured inputs. Following other theoretical works [2, 10, 13, 14, 20], undirected graphs are used in this paper to facilitate the analysis even though real neural systems seem to be directed graphs. The synaptic connections are fixed once a network is specified.

3 Model and Simulation Methods

We use $n = 400$ pulse-coupled leaky integrate-and-fire (LIF) neurons. The i th LIF neuron ($1 \leq i \leq n$) obeys the following dynamics:

$$\dot{x}_i(t) = -\gamma x_i(t) + I_i^{syn}(t) + I_i(t), \quad (1)$$

where $x_i(t)$ is the membrane potential, and γ is the leak rate. When $x_i(t)$ reaches 1, the neuron fires and $x_i(t)$ is reset to the resting potential $x_i(t+0) = 0$. During the absolutely refractory period $\tau' = 0.6$ ms after firing, the

membrane potential stays at the resting potential. With the time delay τ after firing, each connected neuron receives an instantaneous spike with the amplitude ϵ . These feedback interactions define the synaptic input $I_i^{syn}(t)$. The bias current $I_i(t)$ reflects spatiotemporal features of external stimuli. Although homogeneous inputs $I_i(t) = I(t)$ for $1 \leq i \leq n$ easily lead to stable full synchrony [26] that is robust against some heterogeneity [8, 31], sufficiently heterogeneous $I_i(t)$, which we concentrate on, is more concerned with clustered firing or local synchrony.

We define a synchrony measure syn within a group of neurons $\mathcal{S} \subset \{1, 2, \dots, n\}$ [13] by

$$syn(\mathcal{S}) = \sigma \left(\frac{1}{|\mathcal{S}|} \sum_{i \in \mathcal{S}} x_i \right) / \frac{1}{|\mathcal{S}|} \sum_{i \in \mathcal{S}} \sigma(x_i), \quad (2)$$

where $|\mathcal{S}|$ is the cardinality of \mathcal{S} , and the fluctuation $\sigma(x)$ of a temporal waveform x up to time T is given by

$$\sigma(x)^2 = \frac{1}{T} \int_0^T \left(x(t) - \frac{1}{T} \int_0^T x(t') dt' \right)^2 dt. \quad (3)$$

Consequently, syn is normalized between 0 and 1. More synchronous firing gives larger values of syn since the population average of x_i behaves more similarly to each x_i . The values of syn shown in the following figures are the averages based on 25 runs.

We use the Euler algorithm with a time step equal to 0.05 ms for numerical simulations, except when examining robustness of the results against different integration methods in Sect. 5.1.

4 Effect of Spread Vertex Degrees on Synchrony

Here the effect of heterogeneous vertex degrees is examined. In this section, we assume that the inputs are static: $I_i(t) = I_i$, and that I_i are distributed according to the uniform distribution on $[I_0(1 - \Delta_I), I_0(1 + \Delta_I)]$ where $I_0 = 28.5$ and $\Delta_I = 0.08$. Since $I_i > \gamma$, the neurons are oscillatory. We also set $k = 12$, $\epsilon = 0.05$, $\gamma = 25 \text{ ms}^{-1}$, and $\tau = 0.5$ ms.

Figure 2(a) shows how the conventional rewiring (unbalanced rewiring) introduced in Sect. 2 influences the degree of synchrony. To inspect synchrony on various spatial scales, $syn(\mathcal{S})$ averaged over all possible \mathcal{S} that consist of $n' \leq n$ adjacent neurons on the ring substratum are displayed in Fig. 2(a). The best global synchrony ($n' = 400$, the bottom line) is obtained with $p \cong 0.3$, although the peak is not so prominent. This is consistent with the results for coupled Hodgkin-Huxley neurons [13], whereas the optimal values of p are much larger here as for the results for coupled oscillators [2]. For smaller p , traveling waves or clustered states appear. In this situation, as the top line ($n' = 4$) in Fig. 2(a) indicates, neurons locally synchronize owing to the high intragroup connectivity characterized by large $C(p)$, whereas large $L(p)$ prohibits global synchrony. With intermediate values of p , remote neurons communicate rapidly enough via shortcuts to realize global synchrony, and abundant local connections guarantee precise synchrony. Too large values of p result in asynchronous firing.

However, Fig. 2(a) and other theoretical results [2, 13, 14] do not necessarily support biological relevance of small-world networks. Related to synaptic inputs, two desynchronizing factors are identified for networks of homogeneous neurons [8, 28], namely, (i) spatially heterogeneous inputs, and (ii) heterogeneity in the number of inputs to a neuron, or heterogeneous k_v . The positive values of Δ_I and the random rewiring underlie the factors (i) and (ii), respectively. When p is large, the factor (ii) overrides the tendency toward global synchrony caused by small $L(p)$ [10] and that toward local synchrony caused by large $C(p)$, resulting in asynchrony. As a result, the enhanced synchronization with intermediate values of p is not entirely of the topological origin although small-world networks approximate to real neural networks in terms of $L(p)$ and $C(p)$. The vertex degree is homogeneous for $p = 0$ because of the perfect symmetry, whereas that of the random graph ($p = 1$) has the Poisson distribution with mean k [6]. Real neural networks would not have homogeneous k_v no matter whether they are close to regular, small-world, or random networks. It is possible to construct modified graph families whose degree distributions obey the Poisson distribution independent of p [4, 18]. However, here we treat more tractable cases with $k_v = k$ for all the vertices regardless of p because synchrony is more easily attained with more homogeneous networks, especially when networks are small as used in numerical simulations.

Figure 1 compares $L(p)$ and $C(p)$ of the graphs based on the original rewiring procedure (unbalanced random rewiring) and the modified rewiring procedure (balanced random rewiring). To generate balanced networks, we first remove $pkn/2$ edges whose endpoints are denoted by $v_{i,1}$ and $v_{i,2}$ ($1 \leq i \leq pkn/2$) as is done in generating unbalanced networks. Let us denote ρ a randomly chosen permutation on $\{1, 2, \dots, pkn/2\}$. Then new edges are created by connecting $v_{i,1}$ and $v_{\rho(i),2}$ ($1 \leq i \leq pkn/2$). Another permutation is tried if there appear multiple edges, a removed

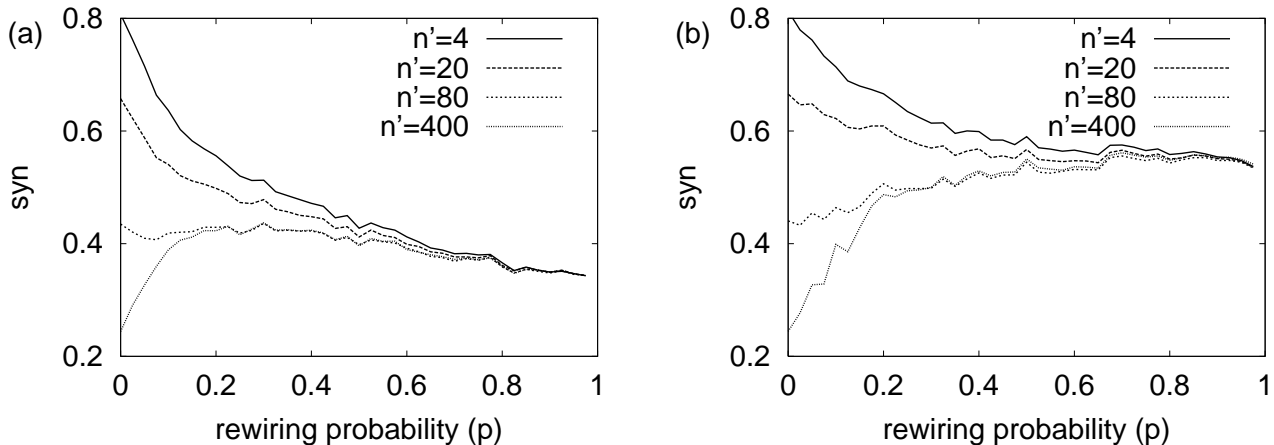


Figure 2: The synchrony measure syn with (a) the unbalanced random rewiring, and (b) the balanced random rewiring. The size of local groups of neurons within which syn is evaluated is denoted by n' .

edge, or self-connection. Insusceptibility of $L(p)$ and $C(p)$ to the graph modification evident in Fig. 1 permits us to explore topological effects on dynamics using the balanced random rewiring.

Degrees of synchrony with the unbalanced and balanced rewiring are compared in Figs. 2(a) and (b). Figure 2(b) shows that the optimal p for synchrony vanishes with the balanced rewiring. Synchrony is induced in original small-world networks when $L(p)$ and the heterogeneity in k_v are simultaneously small. In the balanced networks, however, effects of heterogeneous k_v are abolished. Now, global synchrony just improves as p increases ($n' = 400$, the bottom line) since the contribution of small $L(p)$ in favor of global synchronization surpasses that of small $C(p)$ in favor of desynchronization. By the same token, diffusively coupled neurons do not yield the optimal p in the small-world regime even in the unbalanced networks [33]. This is because the influence of heterogeneous k_v in diffusively coupled networks is less prominent than in pulse-coupled cases.

Locally, rapid communication between pulse-coupled neurons is possible irrespective of $L(p)$ and p . Local synchrony degrades as p increases (see $n' = 4$, the top line) since $C(p)$ rather than $L(p)$ determines the possibility of local synchronization.

5 Synchrony of Remote Neurons with Coherent Inputs

Here we shed light on how the network structure affects local and global synchrony of remote neuronal assemblies. The combined effects of network topology and coherence of inputs to different neurons [3, 9, 19, 20] are also detailed.

5.1 Constant Bias Inputs

We first deal with temporally constant and spatially structured inputs. In relation to feature binding as we discuss in Sect. 7.2, let us assume that two separated neuronal assemblies receive a common bias added to the background level. The assemblies \mathcal{S}_1 and \mathcal{S}_2 are located on the opposite sides of the ring: $I_i = 1.1I_0$ for $i \in \mathcal{S}_1 \cup \mathcal{S}_2$, $\mathcal{S}_1 = \{i; 0 < i \leq 0.1n\}$, and $\mathcal{S}_2 = \{i; 0.5n < i \leq 0.6n\}$. The background activity I_i given to the neurons $\overline{\mathcal{S}} = \{1, 2, \dots, n\} \setminus (\mathcal{S}_1 \cup \mathcal{S}_2)$ is taken randomly from the uniform distribution on $[I_0(1 - \Delta_I), I_0(1 + \Delta_I)]$. We put $\epsilon = 0.05$, $\gamma = 40 \text{ ms}^{-1}$, $I_0 = 38.5 \text{ ms}^{-1}$, $\Delta_I = 0.1$, $\tau = 1.2 \text{ ms}$, and uncorrelated Gaussian white noise with the standard deviation 1.0×10^{-3} per step is applied to all the neurons. Figure 3(a) shows degrees of synchrony of interest, namely, $syn(\mathcal{S}_1)$, $syn(\mathcal{S}_2)$, $syn(\mathcal{S}_1 \cup \mathcal{S}_2)$, and $syn(\mathcal{S}_1 \cup \mathcal{S}_2 \cup \overline{\mathcal{S}})$. Local precise synchrony within \mathcal{S}_1 or \mathcal{S}_2 requires large $C(p)$ associated with small p , with synchrony deteriorating as p increases. On the other hand, the intergroup synchrony is enhanced when $p \in [0.2, 0.5]$, with $syn(\mathcal{S}_1 \cup \mathcal{S}_2)$ significantly larger than $syn(\mathcal{S}_1 \cup \mathcal{S}_2 \cup \overline{\mathcal{S}})$. Intergroup synchrony is difficult when p is too small because large $L(p)$ prohibits \mathcal{S}_1 and \mathcal{S}_2 from communicating fast enough. Intermediate values of p let remote groups of neurons synchronize with the help of shortcuts while local connections necessary to maintain precise intragroup synchrony are still abundant. Although rough global synchrony emerges with larger p , synchrony of the neurons receiving the common inputs is deteriorated because the loss of local connectivity forces these neurons to interact with a random selection of neurons receiving heterogeneous inputs [31].

For $(k, \epsilon) = (8, 0.073)$ and $(k, \epsilon) = (18, 0.035)$ with the other parameter values fixed, the values of syn are shown

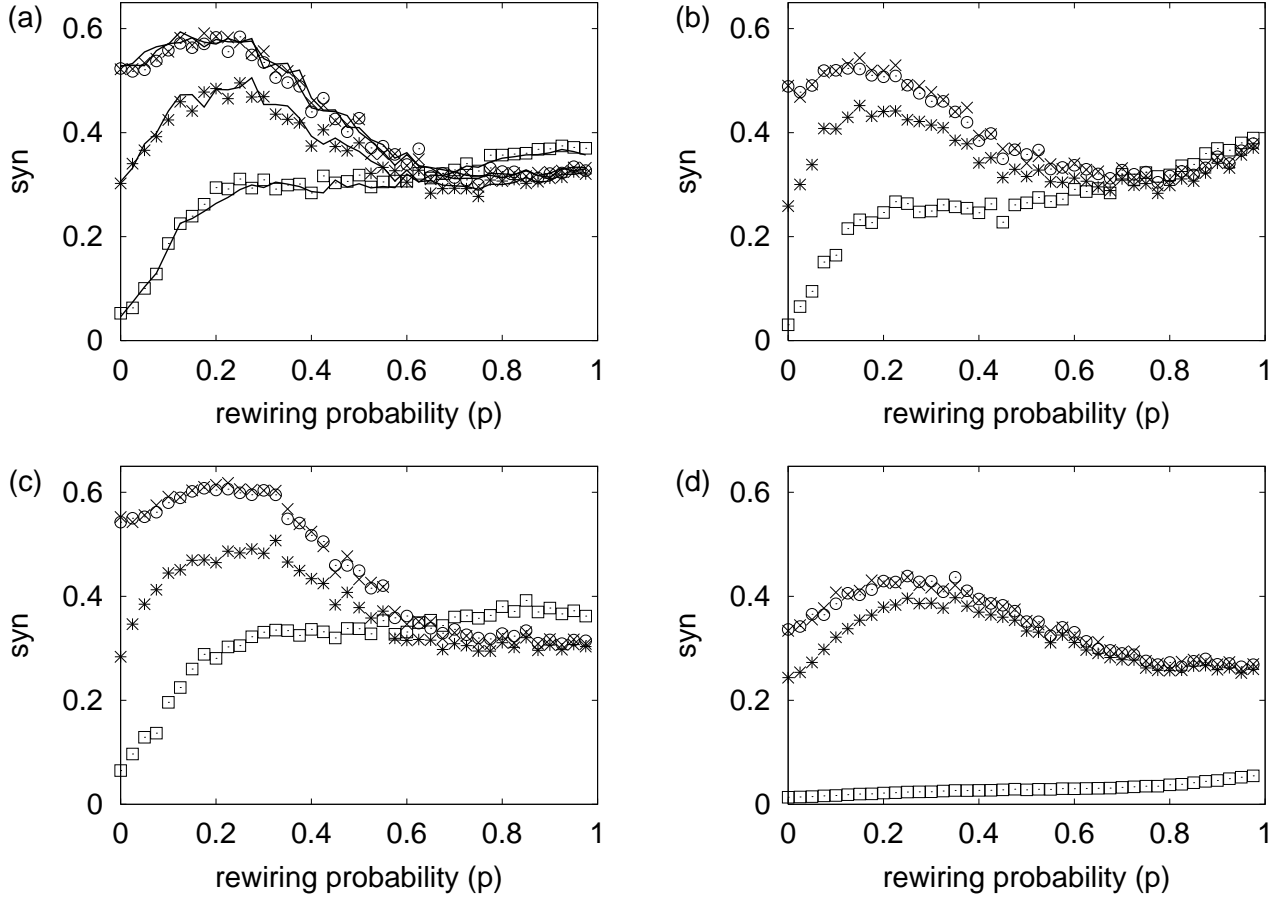


Figure 3: The synchrony measure $syn(\mathcal{S}_1)$ (crosses), $syn(\mathcal{S}_2)$ (circles), $syn(\mathcal{S}_1 \cup \mathcal{S}_2)$ (asterisks), and $syn(\mathcal{S}_1 \cup \mathcal{S}_2 \cup \overline{\mathcal{S}})$ (squares) when two separated coherent stimuli are presented. (a), (b), and (c) are the results for bias inputs with $(k, \epsilon) = (12, 0.05)$, $(8, 0.073)$, and $(18, 0.035)$, respectively. (d) shows the results for correlated noise inputs with $(k, \epsilon) = (12, 0.05)$. The results are obtained by the normal Euler algorithm except those indicated by the solid lines in (a), which are obtained by the improved Euler algorithm.

in Figs. 3(b) and (c), respectively. The firing rates are kept unchanged by modulating ϵ . The values of p for improved intergroup synchrony are robust with respect to k and are larger than those for the small-world regime [2]. The clustering property measured by $C(p)$ is based on the number of connected triangles in the network. Therefore, even though $C(p)$ is small with $p \cong 0.3$ as demonstrated in Fig. 1(b), the local edges within \mathcal{S}_1 or within \mathcal{S}_2 are still abundant enough for intragroup synchrony. Given intragroup synchrony, what promotes intergroup synchrony is the global connections between \mathcal{S}_1 and \mathcal{S}_2 . However, a small value of $L(p)$ reminiscent of the small-world property does not necessarily indicate sufficient global connections. When p is small, the number of global connections increases linearly with p , and $L(p)$ decreases logarithmically with p [32]. Actually, p must be larger than for small-world networks to ensure effective interactions between remote assemblies. In spite of the deviation of the optimal range for p from the small-world regime, improved intergroup synchrony is realized only when the local and global interactions cooperate.

As a remark, numerical results for LIF neurons are generally sensitive to the simulation time step unless firing time is calculated by the appropriate interpolation that the standard Euler algorithm has ignored [11]. The lines in Fig. 3(a) indicate values of syn when the improved Euler algorithm [11] is implemented. The results do not critically depend on the integration methods, which implies the robustness of the results. This is also true for other numerical results in this paper.

5.2 Correlated Noise Inputs

Constant inputs are often too simple to mimic real inputs with a large amount of fluctuation. Additionally, neurons receiving coherent temporally modulated inputs are more likely to synchronize than when receiving coherent constant inputs [15]. Here we use the Ornstein-Uhlenbeck processes to emulate such inputs. The Ornstein-Uhlenbeck process [15, 17] is defined by

$$\frac{dy_i(t)}{dt} = -\frac{y_i(t)}{\tau_{ou}} + \xi_i(t), \quad (4)$$

where we set $\tau_{ou} = 3.0$ ms. Gaussian white noise $\xi_i(t)$ is applied at every time step to emulate the Brownian motion. The spatial inputs simulating two coherent but remote input assemblies are defined by

$$I_i(t) = I_0 + 0.09 y_i(t), \quad (1 \leq i \leq n), \quad (5)$$

where the correlation between $\xi_i(t)$ and $\xi_j(t)$ is 0.8 if $i, j \in \mathcal{S}_1 \cup \mathcal{S}_2$ and 0 otherwise. Figure 3(d) shows the numerical results for the Ornstein-Uhlenbeck inputs. The parameters take the same values as those for Fig. 3(a) except that we set $I_0 = 0.044$ to preserve the firing rates. Enhanced synchrony with intermediate values of p is also observed in this case. A remarkable difference from Fig. 3(a) is that the neurons are globally asynchronous even when p is large. Only the neurons receiving correlated inputs are capable of maintaining synchrony, and the difference in $syn(\mathcal{S}_1 \cup \mathcal{S}_2)$ and $syn(\mathcal{S}_1 \cup \mathcal{S}_2 \cup \bar{\mathcal{S}})$ is ascribed to the correlated inputs [15]. The additional amount of syn when $p \cong 0.3$ owes to global coupling. As a remark, $syn(\mathcal{S}_1)$ and $syn(\mathcal{S}_2)$ significantly decrease for small p compared with the case of constant inputs. This might be because of the relatively short range of the local connections.

6 Degree of Synchrony Modulated by Input Structure

We have seen that distant neurons fire synchronously only when they are stimulated by the coherent constant or coherent noisy inputs. In experiments with visual stimuli, even better synchrony takes place when two remote but coherent inputs are interpreted to be united as one global stimulus [9]. Related to these experimental facts, we examine how inputs with different spatial structure affect spatial firing patterns.

First, three types of bias inputs, namely, (I) a globally coherent input $I_i = 1.1I_0$ for $0 < i \leq 0.6n$, (II) two separated coherent inputs $I_i = 1.1I_0$ for $i \in \mathcal{S}_1 \cup \mathcal{S}_2$, and (III) two locally coherent but globally incoherent inputs $I_i = 1.1I_0$ for $i \in \mathcal{S}_1$ and $I_i = 1.15I_0$ for $i \in \mathcal{S}_2$, are applied. Input (II) is equivalent to one used in Sect. 5.1. The bias I_i to the neurons in the background and the other parameter values are the same as before. As shown in Fig. 4(a), $syn(\mathcal{S}_1 \cup \mathcal{S}_2)$ increases with input (I) and decreases little with an increasing p since the diminishing local communications are compensated by the global connections created by random rewiring, many of which still fall within the range of the global input. On the other hand, the neurons are much less synchronized with input (III) since the global coupling cannot compensate the desynchronizing effects due to the heterogeneous inputs to \mathcal{S}_1 and \mathcal{S}_2 [31].

The corresponding results with the correlated noise inputs introduced in Sect. 5.2 are shown in Fig. 4(b). We assume that the correlation between I_i and I_j is 0.8 only when inputs to the i th and j th neurons are supposed to be coherent. The difference between syn for input (II) and that for (III), which depends little on p , is attributed to the correlated inputs. The additional amount of syn , which is nearly equal to the syn value for input (III), is induced by

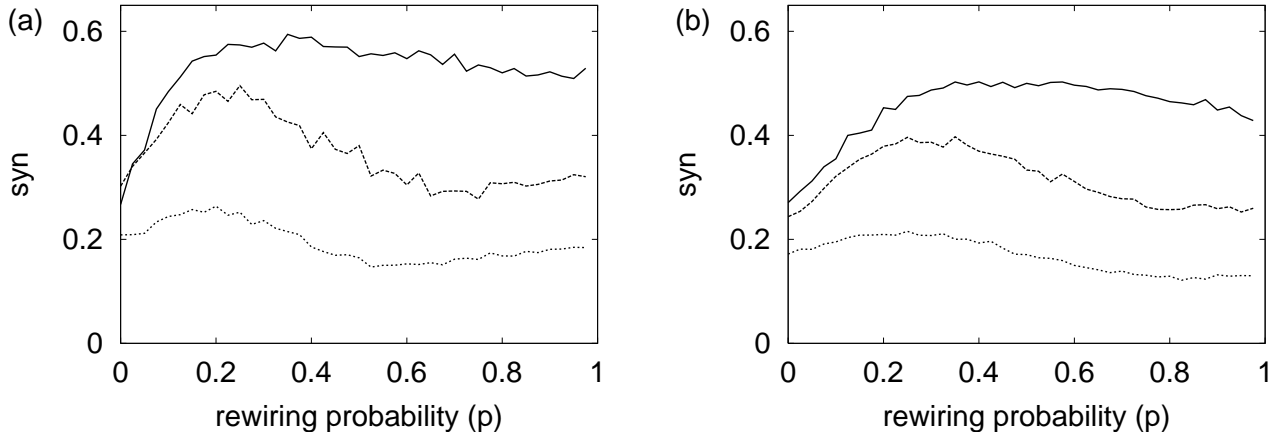


Figure 4: The synchrony measure $syn(\mathcal{S}_1 \cup \mathcal{S}_2)$ when (I) a globally coherent input (solid lines), (II) two separated coherent inputs (dashed lines), and (III) two separated incoherent inputs (dotted lines) are presented. The inputs are applied as (a) biases or (b) correlated noise. We set $k = 12$ and $\epsilon = 0.05$.

the global coupling. This result supports that synchrony is reinforced with intermediate p purely for the topological reason. Input (I) realizes larger syn as expected.

7 Discussion

7.1 Two Modes of Dynamics

Figure 2(b) shows a tradeoff between the temporal precision and the spatial extent of synchrony. For small p , local precise synchrony appears (see the top line), whereas neurons are globally asynchronous (see the bottom line). In this regime, many locally synchronous clusters coexist and can encode inputs with higher spatial resolution. At the extreme, each neuron fires independently of all the others to represent the corresponding $I_i(t)$. By contrast, for large p , syn is almost independent of the group size n' since physical locations of neurons do not make sense; spatiotemporal inputs are encoded crudely in the sense of spatial resolution but robustly. As p increases, rough global synchrony replaces local precise synchrony.

These results contrast with the dual coding in feedforward networks that receive a temporal signal [16, 17, 25]. With strong coupling, a small amount of noise, and homogeneity, neurons synchronize, possibly resorting to rough but power-saving synchronous coding with spatiotemporal cell assemblies [5, pp. 141–173]. This mode is a generalization of the synfire chains [1], [5, pp. 121–140]. With weak coupling, a large amount of noise, and heterogeneity, neurons desynchronize, possibly encoding temporal signals more precisely by the population rate coding. On the other hand, recurrent networks with spatially structured inputs are investigated in this paper. Robust coding with global synchrony and spatially accurate coding with rough precise local synchrony are in the tradeoff relation. The brain may modulate p to switch between the two modes through synaptic plasticity [5, 17, 27, 28].

7.2 Feature Binding

In experiments, when two visual objects moving in the same direction are presented, neurons in the visual cortex receiving the same preferred stimuli fire synchronously even if the neurons are spatially separated [9]. Since the topological structure of receptive fields generally agrees with the anatomical one for example in the primary visual cortex, current biases higher than the background level are often given to two separated groups of neurons to model two objects. With local connections only, nearby objects can be united as a synchronous cluster by intergroup interaction, but presentation of remote objects does not allow global intergroup synchrony [12, 30]. More elaborated networks with local excitations and global uniform inhibitions realize cluster coding in which different objects are encoded by separated synchronous groups that fire alternatively [24, 29].

We have shown that the cooperation of the local and global interactions, which is realized by intermediate values of p , facilitates synchrony among remote groups of neurons. The combined effects of couplings and coherent inputs have also been emphasized. The results may be relevant to binding of remote coherent stimuli such as visual object segmentation [24, 31], the synfire chain [1], and dynamical cell assembly [7], although we have ignored the diversity

of the stimulus preferences of individual neurons such as orientation selectivity and simply represented a coherent object as a common signal with a spatial structure. Also in terms of network topology, our results are consistent with the findings that nearby neurons with overlapping receptive fields are densely and strongly connected irrespective of preferred stimuli, while weak long-range connections exist only between the neurons with the common preferred stimuli [19].

Another point to be noted is that the occurrence of synchrony is unrelated to the locations of external inputs as long as they are coherent. Other model studies of feature binding require closeness of objects [12, 30], homogeneous global inhibitors [24, 29], or the stimulus-dependent synaptic strength that changes rapidly [19, 20, 29]. Our neural networks with the cooperative local and global connections do not rely on these requirements that may be biologically too strong.

7.3 On Plausibility of Using Small-world Networks

With our results, we do not insist that small-world networks naturally emerges to facilitate synchrony or information processing. As Fig. 4 shows, separation of three kinds of inputs (I), (II), and (III) in Sect. 6 is also achieved with larger p . The purpose in the analysis in Sects. 5 and 6 was to examine the topological effect on synchrony and manifest the cooperation of couplings and inputs. Randomly rewired networks including small-world networks are used just for the same goal. For example, synfire chains [1], [5, pp. 121–140] in which precise local synchrony as well as global information transmission is essential may be related to rewired networks with intermediate values of p [13]. However, random rewiring always discards topological information. Real neural networks may have particular structures and inherent correlations as a result of learning even if $L(p)$ and $C(p)$ resemble those of randomly shuffled small-world networks [4]. To consider learning, dynamics of synaptic connectivities, and also inhibitory couplings is an important future problem.

Acknowledgements

We thank M. Watanabe, Y. Tsubo, and C. van Leeuwen for helpful discussions. This work is partially supported by the Japan Society for the Promotion of Science and by the Advanced and Innovational Research program in Life Sciences and a Grant-in-Aid No.15016023 on priority areas (C) Advanced Brain Science Project from the Ministry of Education, Culture, Sports, Science, and Technology, the Japanese Government.

References

- [1] Abeles M (1991) Corticonics. Cambridge University Press, Cambridge.
- [2] Barahona M, Pecora LM (2002) Synchronization in small-world systems. *Phys Rev Lett* 89(5): 054101
- [3] Ben-Yishai R, Lev Bar-Or R, Sompolinsky H (1995) Theory of orientation tuning in visual cortex. *Proc Natl Acad Sci USA* 92: 3844–3848
- [4] Callaway DS, Hopcroft JE, Kleinberg JM, Newman MEJ, Strogatz SH (2001) Are randomly grown graphs really random? *Phys Rev E* 64: 041902.
- [5] Domany E, van Hemmen JK, Schulten K (Eds.) (1994) Models of neural networks II. Springer-Verlag, New York.
- [6] Erdős P, Rényi A (1959) On random graphs. *Publicationes Mathematicae* 6: 290–297.
- [7] Fujii H, Ito H, Aihara K, Ichinose N, Tsukada M (1996) Dynamical cell assembly hypothesis – theoretical possibility of spatio-temporal coding in the cortex. *Neural Netw* 9(8): 1303–1350
- [8] Golomb D, Hansel D (2000) The number of synaptic inputs and the synchrony of large, sparse neuronal networks. *Neural Comput* 12: 1095–1139.
- [9] Gray CM, König P, Engel AK, Singer W (1989) Oscillatory responses in cat visual cortex exhibit inter-columnar synchronization which reflects global stimulus properties. *Nature* 338: 334–337
- [10] Guardiola X, Díaz-Guilera A, Llas M, Pérez CJ (2000) Synchronization, diversity, and topology of integrate and fire oscillators. *Phys Rev E* 62(4): 5565–5570

- [11] Hansel D, Mato G, Meunier C, Neltner L (1998) On numerical simulations of integrate-and-fire neural networks. *Neural Comput* 10: 467–483
- [12] König P, Schillen TB (1991) Stimulus-dependent assembly formation of oscillatory responses: I. synchronization. *Neural Comput* 3: 155–166
- [13] Lago-Fernández LF, Huerta R, Corbacho F, Sigüenza JA (2000) Fast response and temporal coherent oscillations in small-world networks. *Phys Rev Lett* 84(12): 2758–2761
- [14] Lago-Fernández LF, Corbacho FJ, Huerta R (2001) Connection topology dependence of synchronization of neural assemblies on class 1 and 2 excitability. *Neural Netw* 14: 687–696
- [15] Mainen ZF, Sejnowski TJ (1995) Reliability of spike timing in neocortical neurons *Science* 268: 1503–1506
- [16] Masuda N, Aihara K (2002) Bridging rate coding and temporal spike coding by effect of noise. *Phys Rev Lett* 88(24): 248101
- [17] Masuda N, Aihara K (2003) Duality of rate coding and temporal coding in multilayered feedforward networks. *Neural Comput* 15: 103–125
- [18] Molloy M, Reed B (1995) A critical point for random graphs with a given degree sequence. *Random Struct Algorithms* 6: 161–180
- [19] Sompolinsky H, Golomb D, Kleinfeld D (1990) Global processing of visual stimuli in a neural network of coupled oscillators. *Proc Natl Acad Sci USA* 87: 7200–7204
- [20] Sompolinsky H, Golomb D, Kleinfeld D (1991) Cooperative dynamics in visual processing. *Phys Rev A* 43(12): 6990–7011
- [21] Sporns O, Tononi G, Edelman GM (2000) Theoretical Neuroanatomy: relating anatomical and functional connectivity in graphs and cortical connection matrices. *Cerebral Cortex* 10: 127–141.
- [22] Steinmetz PN, Roy A, Fitzgerald PJ, Hsiao SS, Johnson KO, Niebur E (2000) Attention modulates synchronized neuronal firing in primate somatosensory cortex. *Nature* 404: 187–190
- [23] Stephan KE., Hilgetag C-C, Burns GAPC, O’Neill MA, Young MP, Kötter R (2000) Computational analysis of functional connectivity between areas of primate cerebral cortex. *Phil Trans R Soc Lond B* 355: 111–126
- [24] Terman D, Wang D (1995) Global competition and local cooperation in a network of neural oscillators. *Physica* 81D: 148–176
- [25] van Rossum MCW, Turrigiano GG, Nelson SB (2002) Fast propagation of firing rates through layered networks of noisy neurons. *J Neurosci* 22(5): 1956–1966
- [26] van Vreeswijk C (1996) Partial synchronization in populations of pulse-coupled oscillators. *Phys Rev E* 54(5): 5522–5537
- [27] van Vreeswijk C, Sompolinsky H (1996) Chaos in neuronal networks with balanced excitatory and inhibitory activity. *Science* 274: 1724–1726
- [28] van Vreeswijk C, Sompolinsky H (1998) Chaotic balanced state in a model of cortical circuits. *Neural Comput* 10: 1321–1371
- [29] von der Malsburg Ch, Schneider W (1986) A neural cocktail-party processor. *Biol Cybern* 54: 29–40
- [30] Wang D (1995) Emergent synchrony in locally coupled neural oscillations. *IEEE Trans on Neural Netw* 6(4): 941–948
- [31] Wang XJ, Buzsáki G (1996) Gamma oscillation by synaptic inhibition in a hippocampal interneuronal network model. *Journal of Neurosci* 26(20): 6402–6413
- [32] Watts DJ, Strogatz SH (1998) Collective dynamics of ‘small-world’ networks. *Nature* 393: 440–442
- [33] Watts DJ (1999) *Small worlds*. Princeton University Press, Princeton